Ground Motion Accelerograms for Nonlinear Time History Analysis in Low-to-Moderate Seismicity Regions

Yiwei Hu[1,4], Nelson Lam[2,4], Scott Menegon[3,4]

1. Corresponding Author. PhD candidate, Department of Infrastructure Engineering, The University of Melbourne, Parkville, VIC 3010, Australia.
   Email: huyh1@student.unimelb.edu.au

2. Professor, Department of Infrastructure Engineering, The University of Melbourne, Parkville, VIC 3010, Australia. Email: ntkl@unimelb.edu.au

3. Research Fellow, Centre for Sustainable Infrastructure, Swinburne University of Technology, Melbourne, Australia. Email: smenegon@swin.edu.au

4. Bushfire and Natural Hazard Cooperative Research Centre, Melbourne, Australia

Abstract

This paper is concerned with selecting and scaling records of earthquake ground motion acceleration time histories for use in southeastern Australia which is used as an example to illustrate the application of the Conditional Mean Spectra (CMS) methodology in a low to moderate seismicity region. The study involved making use of a diversity of Ground Motion Prediction Equations (GMPEs) along with a recently developed regional-adjustable Component Attenuation Model (CAM) which takes into account effects of the regional crustal profile on ground motion behavior. When applying the GMPEs to construct the CMS for bedrock conditions three different combinations of weighting factors were adopted to generate three ensembles of accelerograms on bedrock. Differences among the three accelerogram ensembles have been found to be minor. Ground motion accelerograms to represent the conditions of some example soil sites have been generated accordingly for engineering research and for supporting the design of critical infrastructure.

Keywords: GMPEs, Component Attenuation Model, Conditional Mean Spectra

1. INTRODUCTION

In regions of low to moderate seismicity earthquake ground motion accelerograms are rarely required in seismic design or assessment of structures. However, there were occasions when accelerograms were sought for constructing site-specific response spectra or for supporting the design of critical facilities. The Pacific Earthquake Engineering Research (PEER) ground motion database based at University of California, Berkeley, provides online resources for downloading accelerograms for use in research or in engineering practices. To select and scale accelerograms using the database, a target elastic response spectrum would need to be specified. A uniform hazard spectrum (UHS) as developed from Probabilistic Seismic Hazard Analysis (PSHA) can be the target spectrum for selecting and scaling accelerograms. Alternatively, a design response spectrum as stipulated by the standard may also be specified as the target spectrum. As is widely recognized it can be overly conservative to specify a UHS or a Code spectrum as target spectrum because of their very broad band nature given that these response spectra have incorporated many possible earthquake scenarios contributing to the predicted seismic hazard of a site. The short period part of UHS is normally dominated by small-magnitude earthquakes at close range whereas the long period part of the spectrum is mainly contributed by larger magnitude seismic events at longer distances. Thus, no single earthquake event on its own can possibly have its response spectrum matching the UHS at all considered periods. As pointed out by Baker (2010) a scenario specific, or event specific, response spectrum would more realistically represent the condition of one earthquake event and hence is less conservative than a UHS or a code spectrum. Thus, dominating earthquake scenarios would need to be identified. The identified scenarios can be used to predict event specific response spectra each of which is to be scaled to match the UHS/Code spectrum at a pre-determined reference natural period of vibration (T^*). Ground motion prediction equations (GMPEs) representative of regional conditions are required to serve this scaling process. The constructed event specific target spectrum which is also known as the conditional mean spectrum (CMS) can be used to build ensembles of ground motion accelerograms representing bedrock conditions (i.e. Class B sites). The bedrock excitations can in turn be used for generating site specific ground motions and response spectra for a range of site classes to serve earthquake engineering research and to support the design of critical infrastructure.

Research undertaken by Baker (2010 and 2015) established a methodology for constructing suitable CMSs based on the procedure outlined in the above. However, adapting the methodology of Baker in a low to moderate seismicity region is not straightforward in view of uncertainties over ground motion modelling and identification of a few dominating earthquake scenarios. This study represents an attempt to adapt the methodology for use in a stable (intraplate) region using southeastern Australia (SEA) as an example. Adapting the CMS methodology for use in an intraplate area has not been dealt with in any published guidelines and the challenges are mostly described in this article. For example, in a region lacking indigenous instrumented data, it is always uncertain which GMPE would be suitable for representing regional conditions. When multiple GMPEs have been selected into the study the weighted average GMPE may be used to construct scenario specific response spectra. However, assigning suitable weighting factors to individual GMPE in a rational manner presents another challenge. In the original CMS methodology a UHS is used to identify the dominating earthquake scenarios by de-aggregation analysis for the target sites. However, following this procedure can be problematic in situations where the target response spectrum was not derived from any PSHA

but was instead determined from engineering judgement. This is the case with SEA as the design response spectrum stipulated by the current edition of the Australian standard for seismic actions (AS1170.4 – 2018) features a minimum design hazard factor (Z) of 0.08 which was not based on the results of a PSHA. The objective of this paper is to present the aforesaid challenges and the manner in which these challenges were attended to and overcome.

2. CONSTRUCTING THE CONDITIONAL MEAN SPECTRUM

In this section, the process of constructing the CMS that is representative of the conditions of SEA is described. To construct a CMS there are three key decisions to make: (i) choosing a code design response spectrum as the basis of scaling a CMS, (ii) shortlisting GMPEs that are representative of the conditions of SEA taking into considerations the seismo-tectonic environment and the crustal condition of the region, and (iii) deciding on the design earthquake scenarios each of which is expressed in terms of the magnitude-distance (M-R) combinations. Details of the various components of the CMS construction process as outlined in the above are to be described in the rest of this section.

2.1 CAM and the four other shortlisted GMPEs

In active regions of high seismicity like Western North America (WNA), complete and high-precision earthquake accelerogram records covering a range of magnitude-distance combinations and site classifications might be available for deriving an empirical GMPE by regression analysis. In intraplate regions where strong motion data are lacking, a viable way of modelling ground motions is employing stochastic simulation of the seismological model. This ground motion modelling approach which was first developed in the 1980's (e.g. Boore, 1983) has been the most commonly adopted approach in Eastern North America (ENA) for decades. Seismological models are valuable as they contain authentic information on ground motion behavior in stable continental regions. Importantly, the effects of the source, path and site on ground motion behavior can be decoupled. Thus, regional crustal conditions on the frequency behavior of the earthquake can be represented by frequency dependent scaling factors. What is needed to derive regional specific crustal factors is the shear wave velocity profile of the earth crust down to several kilometers deep. Thus, no strong motions that are captured locally are required. Whilst seismological modelling has been receiving a great deal of attention in seismological research the developed ground motion models cannot be used straightaway for engineering application. It would be necessary to have accelerogram records simulated by use of the model in order that GMPEs can be calculated from the simulated motions.

The more recently developed hybrid empirical approach (e.g. Campbell, 2003) or the referenced empirical approach (e.g. Atkinson, 2008) are innovative tools that integrate the use of seismological modelling with conventional GMPEs. The CAM model is another useful tool which was first introduced by Lam et al. (2000) and further developed by Tang et al. (2019) for transforming Ground Motion (seismological) Models into GMPEs. CAM is found on the principles that a range of mechanisms controlling the intensity of earthquake ground shaking can be modeled individually in order that regional differences can be represented by differences in various component factors: the source, path and crustal factors. CAM employs the source model of the Generalised Additive Double-Corner Frequency (ADCF) form as developed by Boore, Alessandro & Abrahamson (2014) alongside California "sag" parameters (Atkinson & Silva,

2000) to define scaling in the frequency domain and a (less steep) geometric spreading rate of R^{-1}. The crustal factors in SEA were derived in accordance with the local crustal shear wave velocity profiles as reported in Tang and coworkers (2019). The expressions and coefficients of CAM are presented in Appendix A. To validate the source component factor of CAM, the crustal components had to be temporarily removed in order that response spectral accelerations (RSA) predicted from CAM (without-crustal effects) could be compared against predictions from GMPEs of ENA where crustal effects are on the whole very minor and more so for hard-rock sites in ENA (NEHRP site class A, 1996).

In a review study by Ogweno and Cramer (2014), a ranked list of GMPEs representing ENA conditions was compiled. The ranking was determined by benchmarking against ground motions that had been archived in the New Generation Attenuation – East (NGA-East) ground motion database of 2014. The three top-ranked GMPEs are namely: PZT11 (Pezeshk, Zandieh & Tavakoli, 2011), AB95 (Atkinson & Boore, 1995) and AB06 (Atkinson & Boore, 2006). In addition, two well-known and recently developed GMPEs: SP14 (Shahjouei & Pezeshk, 2015) and YA15 (Yenier & Atkinson, 2015) that were not in the compiled list have also been included in the study. Table 1 presents the listing of the GMPEs along with values of the key parameters. Response spectra predicted by the shortlisted models for two earthquake scenarios (M5 R = 10 km and M6 R = 30 km) are presented in Figure 1.

Table 1 Approaches and Input Parameters in 5 ENA GMPEs and CAM-without-Crust

GMPEs	Method	Stress Parameter (bars)	Geometric Spreading[1]	Crustal Effect
AB95	Point Source Stochastic Simulation	180	R^{-1}	No
AB06	Finite Fault Model	140	$R^{-1.3}$	Yes[2]
PZT11	Hybrid Empirical Method	250	$R^{-1.3}$	Yes[2]
SP14	Hybrid Empirical Method	250	$R^{-1.3}$	Yes[2]
YA15	Hybrid Empirical & Referenced Empirical Method	250	$R^{-1.3}$	Yes[2]
CAM-without-Crust	Point Source Stochastic Simulation	180	R^{-1}	No

[1] The geometric spreading rate listed refers to short distance within 50 km
[2] The crustal effect in ENA regions are minor because of the hard rock condition

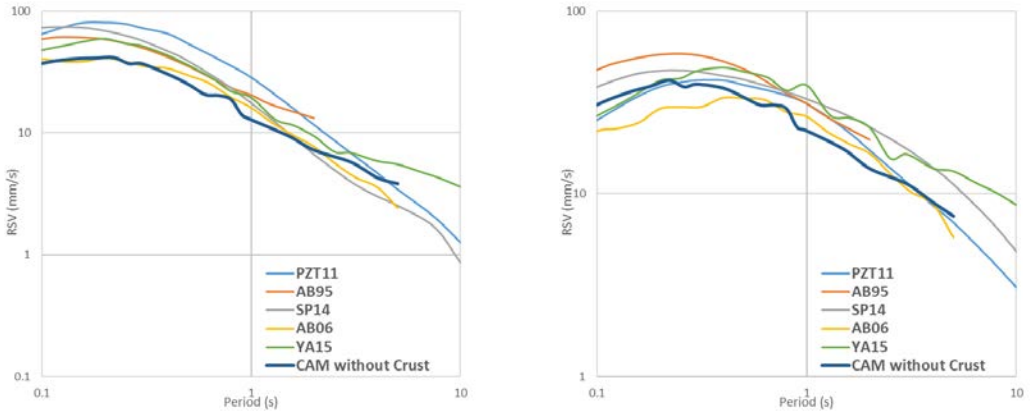

(a) M5 R = 10 km **(b) M6 R = 30 km**

Figure 1 Comparison between CAM-without-Crust and GMPEs of ENA

In Figure 1, the difference between CAM-without-Crust and AB95 can be explained by their respective diverse source models noting that AB95 incorporates a more conservative A93 source model (Atkinson, 1993) compared with the more recently developed ADCF source model (which is based on a stress parameter of 180 bars). Predictions by AB06, PZT11 and SP14 are also moderately higher than predictions by CAM-without-Crust because the crustal effects, however minor, could amplify seismic wave intensity at all periods (by around 20% at $T = 1s$ and 10% at $T = 2s$). Another factor that has aroused much controversy amongst investigators involved in ground motion modelling is the rate of geometrical spread of energy (being $R^{-1.3}$ in PZT11, SP14 and YA15) and their associated tradeoffs with the stress parameter in the source factor. It is shown that the version of CAM as described (CAM-without-Crust which only incorporates the source factor of an intraplate earthquake) provides reasonable predictions for both earthquake scenarios as the predicted response spectrum is reasonable as is within the cluster of predictions by the most well recognized GMPEs of ENA.

The next step in the modelling process is to incorporate suitable crustal factor into CAM in order to extend its use outside ENA (to SEA) where crustal modifications can be significant. The crustal factor is the product of three component factors. The upper crustal amplification factor γ_{am} accounts for the frequency dependent amplification of the seismic shear waves in their transmission within the earth crust of gradually decreasing hardness which is controlled by the shear wave velocity profile (and is characterised by parameter $V_{s,30}$, which is the average shear velocity over the upper 30 m of rock crust). The attenuation of the upper crust γ_{an}, indicated by the frequency cutoff f_{max} or shape factor kappa k_0, counteracts the amplification effects and diminishes spectral amplitudes at high frequencies. The last component is referred to as the mid-crust modification effect that takes into account the difference of the shear wave velocity in the vicinity of the source (V_8). Details of the crustal factor adopted by CAM for SEA are not presented herein and can be found in Tang et al. (2019).

Predictions from CAM for SEA are then compared with that from two locally developed GMPEs: A12 (Allen, 2012) and SGC09 (Somerville et al., 2009), both of which were recommended by Geoscience Australia to be representative of conditions in SEA. The A12 model was developed from results obtained from the analysis of records of 75 local earthquakes of magnitude ranging from M2.8 to M5.4 (with most events having a magnitude in the range M3 to M4). The SGC09 model adopted the source scaling relations of Western Australia and that of Western North America (WNA). The A12 model adopted depth dependent stress parameters: 230 bars (A12-Shallow) and 500 bars (A12-Deep). The list of some key seismological parameters associated with CAM, A12 and SGC09 are listed in Table 2. Comparisons of the Response Spectral Velocity (RSV) predicted from these four GMPEs are presented in Figure 2 which demonstrates overall good agreement between their predictions. It is demonstrated further in Figure 3 that CAM would be able to reach good agreement with A12-shallow if the stress parameter value was revised to 100 bars which is much lower than what is expected of an intraplate earthquake. This is evident of A12 understating ground motion intensities of a future intraplate earthquake which is of magnitude exceeding M5.

Table 2 Seismological Parameters in 2 SEA GMPEs and CAM

GMPEs	Stress Parameter (bars)	Geometric Spreading*	Kappa	$V_{s,30}$ (m/s)	V_8 (km/s)
CAM	200	R^{-1}	0.033	760	3.5
A12-Shallow	230	$R^{-1.33}$	0.006	830	3.6
A12-Deep	500	$R^{-1.33}$	0.006	830	3.6
SGC09	N/A	N/A	0.04	865	N/A

Macro-seismic intensity information expressed in terms of Modified Mercalli Intensity (MMI) has been document in iso-seismal maps for earthquakes occurring within the Australian continent over the past century (McCue, 1995). The part of the MMI database that has been incorporated into the study is listed in Table 3. The reported MMI values were used to infer on RSV values using Eq. (1) and (2) (Lam, Wilson & Tsang, 2010; Atkinson & Kaka, 2007). The comparison between the recorded MMI values and those estimated using CAM is presented in Figure 4 showing reasonable agreement.

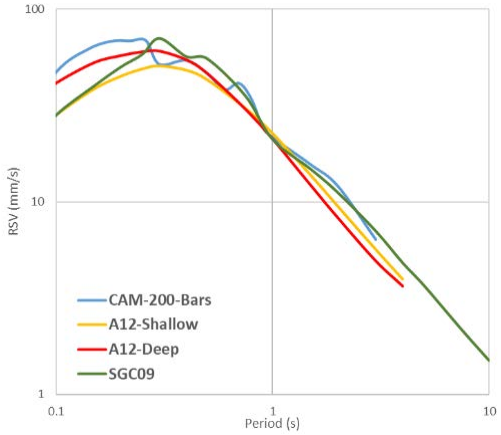

(a) M5 R = 10 km

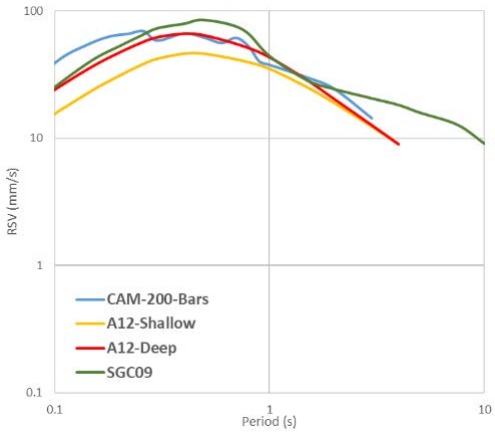

(b) M6 R = 30 km

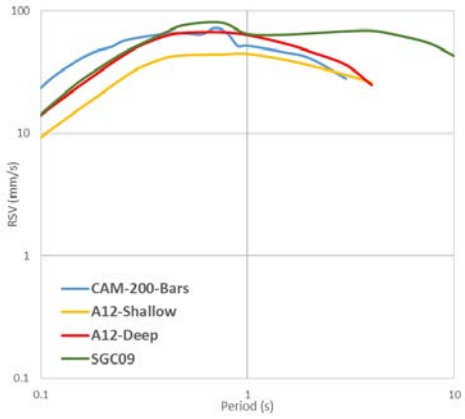

(c) M7 R = 100 km

Figure 2 RSV Comparison between CAM and two GMPEs of SEA

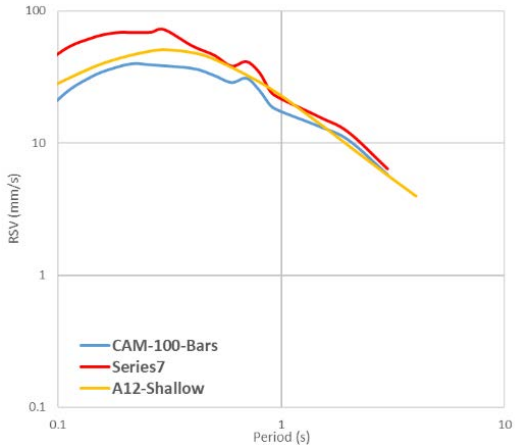

(a) M5 R = 10 km

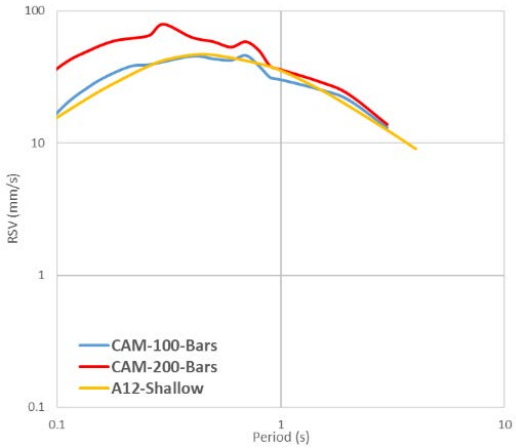

(b) M6 R = 30 km

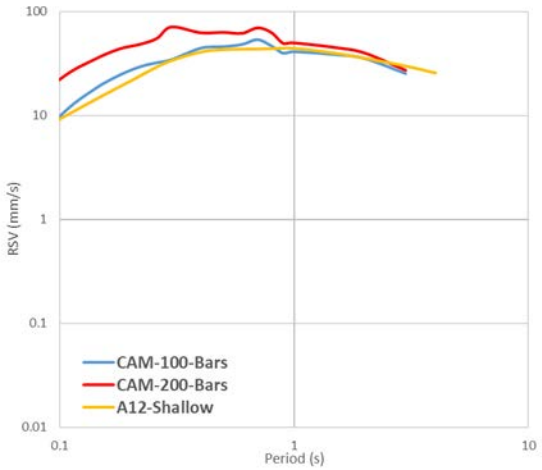

(c) M7 R = 100 km

Figure 3 RSV Comparison between CAM and GMPE (A12-Shallow)

Table 3 Recorded SEA MMI Data and Event Scenarios

Location	Year	Mw	R (km)	Recorded MMI
VIC				
Boolarra/South Gippsland	1969	5.0	10	6
			50	4
Warrnambol/Otway Basin	1903	5.0	5	7
			20	5
			50	4
NSW				
Newcastle	1989	5.4	15	6
			50	5
			100	4

Picton	1973	5.9	40	5
Gunning	1934	5.3	10	6.5
			30	5
			100	4
Maitland	1868	5.0	10	6
SA				
Adelaide	1954	5.1	15	6
			30	5
			120	4
Motpena/Nilpena	1939	5.5	10	6.5
			20	6
			80	5
			180	4

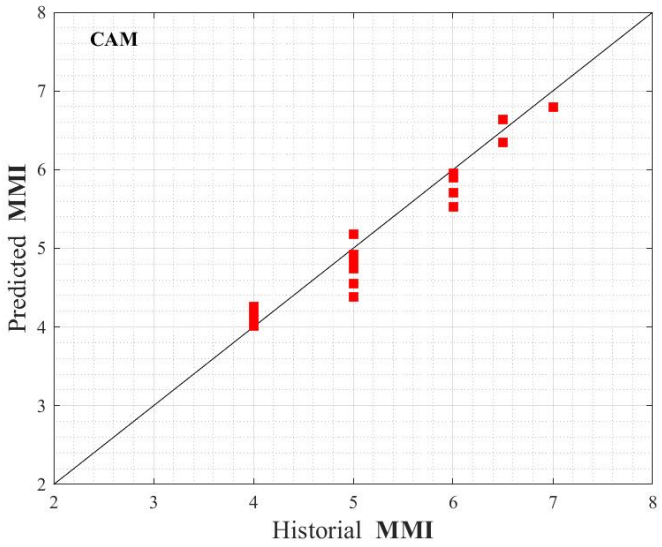

Figure 4 Recorded MMI Versus Predicted MMI from CAM

$$PGV = \max(RSV)\,/1.8 \qquad \text{Eq. (1)}$$

$$MMI = \begin{cases} 4.37 + 1.32 \times \log PGV + 0.47 - 0.19 \times M + 0.26 \times \log R & \log PGV \leq 0.48 \\ 3.54 + 3.03 \times \log PGV + 0.47 - 0.19 \times M + 0.26 \times \log R & \log PGV > 0.48 \end{cases} \qquad \text{Eq. (2)}$$

Further evaluation work has been undertaken based on comparing predictions of CAM for SEA with that from four other GMPEs for three earthquake scenarios: M5 R = 10 km , M6 R = 30 km and M7 R = 100 km. Predictions from these models are in overall agreement but there are discrepancies: predictions by A12 is the lowest whereas predictions by CAM and SGC09 are on the high side.

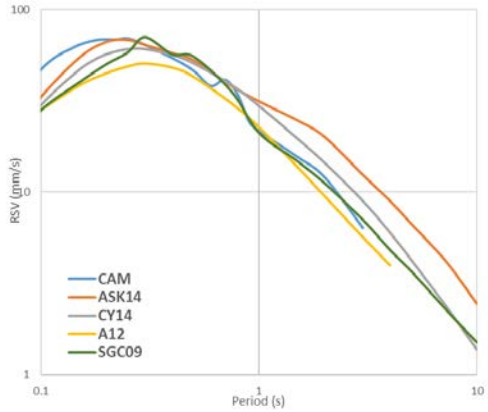

(a) M5 R = 10 km

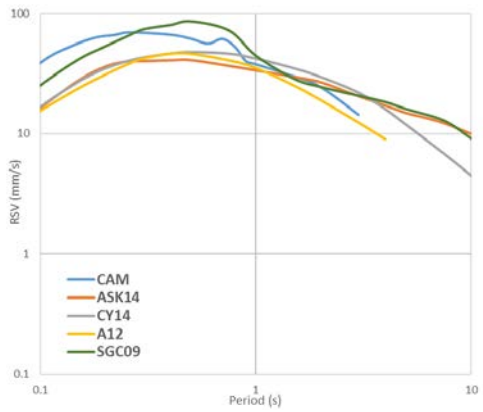

(b) M6 R = 30 km

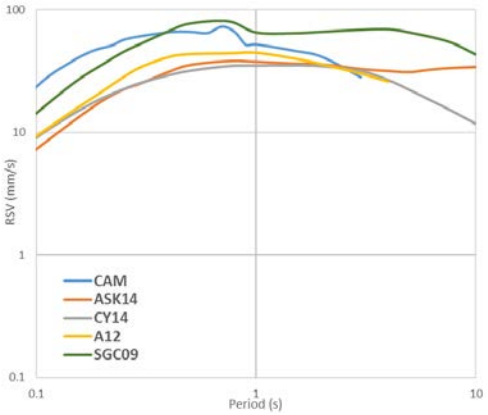

(c) M7 R = 100 km

GMPEs	Source
CAM	This study and Tang et al., 2019
A12	Allen, 2012
SGC09	Somerville et al., 2009
ASK14	Abrahamson, Silva & Kamai, 2014
CY14	Chiou & Young, 2014

Figure 5 Comparison of predictions by selected GMPEs

2.2 Dominant Earthquake Scenarios

In this study the design response spectrum that is stipulated by the current edition of the Australian Standard for seismic actions (AS1170.4 - 2018) is used in place of a UHS. Thus, the code spectrum is not based on a PSHA and no de-aggregation analyses can be undertaken in the usual manner to identify the dominant earthquake scenarios. A global survey on the rate of occurrence of intraplate earthquakes exceeding the magnitude threshold of M5 in the past fifty years (Lam et al, 2016) transpired into the development of an intraplate earthquake recurrence model of the Gutenberg-Richter (G-R) form as shown in Eq. (3), which is based on the assumption of uniform spatial distribution of seismic activities on land.

$$\log_{10} N = 5.2 - 0.9M \qquad \text{Eq. (3)}$$

where N is the number of events exceeding magnitude M in one million square kilometers landmass in every 50 years.

As the development of the uniform seismicity model involved PSHA the contributing earthquake scenarios are known to the authors (refer Figure 6 for results of de-aggregation for natural period of 0.18s). There are no distinctive dominating scenarios but earthquakes with magnitude M5 – M5.5 from 10 – 15 km is shown to contribute most to the low period hazards of around 0.2 seconds whereas larger magnitude longer distance events tend to dominate higher period hazards.

Decisions on the construction of the CMS are summarized as follows:

(1) The response spectrum model used for scaling is the design response spectrum stipulated by Class B sites for $k_p Z = 0.12$ for return period of 2500 years (which corresponds to the minimum hazard factor of $Z = 0.08$).

(2) The reference periods of interests are: 0.18s, 0.5s and 1s to cover a range of structural requirements.

(3) Earthquake magnitudes ranging from M4 to M7 and distances ranging from 5 km to 100 km are within the scope of considerations.

(4) Three schemes of applying weighting factors to the five GMPEs have been attempted. In *Scheme 1*, each GMPE carries an equal weight of 20%. In *Scheme 2*, CAM which makes relatively conservative predictions at the low period range carries a higher weighting of 60% whereas the other GMPEs were each assigned a 10% weighting. In *Scheme 3,* 60% weighting is assigned to A12 which gives lower predictions than the other GMPEs.

Table 4 in below presents a summary of the three weighting schemes as discussed.

Table 4 Dominant Earthquake Scenarios for the three referenced natural periods

Weighting Scheme	GMPEs Weight	Period of Interest (s)		
		0.18	0.5	1
Scheme 1	20% each for CAM, A12, SGC09, ASK14, CY14	M5.5 R15[1]	M6 R20[2]	M6.5 R55[34]
Scheme 2	60% for CAM and 10% each for A12, SGC09, ASK14, CY14			
Scheme 2	60% for A12 and 10% each for CAM, SGC09, ASK14, CY14			

[1] This combination is based on M5.4R16 in Scheme 1, M5.4R18 in Scheme 2 and M5.3R12 in Scheme 3;
[2] This combination is based on M5.9R20 in Scheme 1, M6.0R23 in Scheme 2 and M5.8R17 in Scheme 3;
[3] This combination is based on M6.2R22 in Scheme 1, M6.3R24 in Scheme 2 and M6.2R19 in Scheme 3;
[4] This combination is adjusted to rise the probability of occurring.

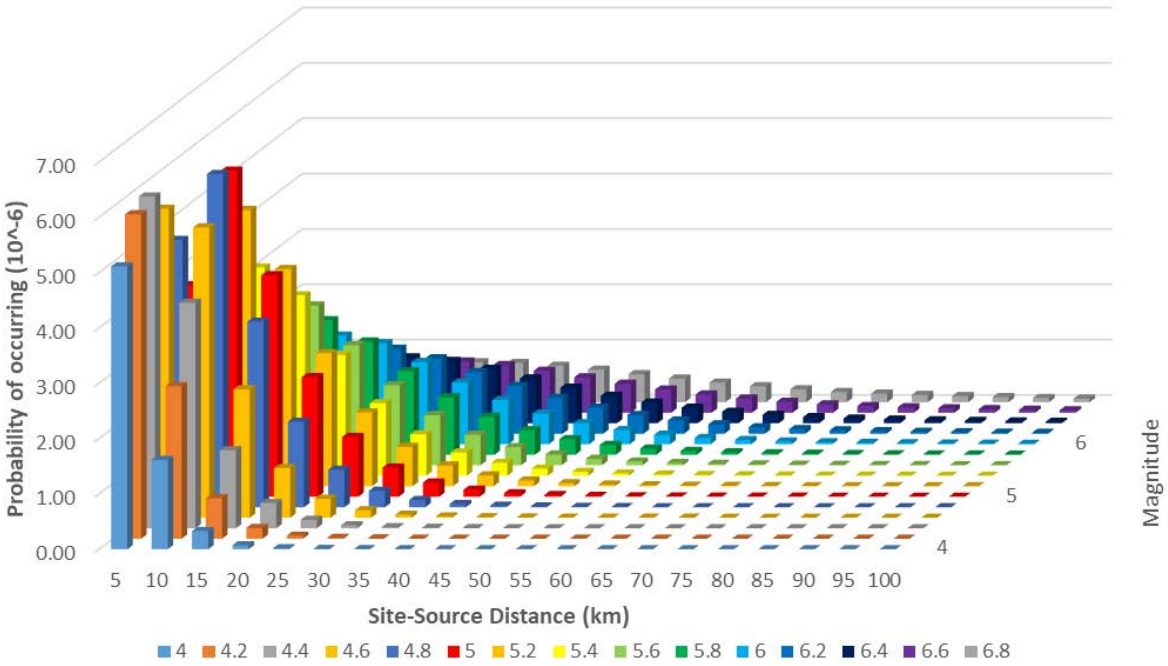

Figure 6 Probability of occurrence at T = 0.18 s (GMPEs Weighting Scheme 1)

2.3 Construction of CMS

The first step of constructing CMS is to first identify the dominating earthquake scenarios. The median response spectrum predictions as the weighted average GMPE is named herein as the scenario-specific spectrum. Parameter ϵ denotes the number of standard deviations that are added to the spectral value predicted by the median response spectrum in order to match with code spectrum at the respective reference periods. The scaling up of the median spectrum produces the "mean plus ϵ σ ". The CMS is then derived by scaling this spectrum using the scaling factor ρ as defined by Eq. (4) which was derived by Baker and Cornell (2006). The CMS which can be defined mathematically by Eq. (5) is essentially a response spectral representation of an earthquake event, and is therefore also known as the event-specific response spectrum. Three scenario-specific and event-specific (CMS) response spectra corresponding to the *Scheme 1* weighting factors are presented in Figure 7 for the reference periods of 0.18s, 0.5s and 1s.

$$\rho_{\ln Sa(T_1),\ln Sa(T_2)} = 1 - \cos\left(\frac{\pi}{2} - (0.359 + 0.163 I_{(T_{min}<0.189)} \ln\frac{T_{min}}{0.189}) \ln\frac{T_{max}}{T_{min}}\right) \quad \text{Eq. (4)}$$

$$\mu_{\ln Sa(T_2)|\ln Sa(T_1)=\ln Sa(T_1)^*} = \mu_{\ln Sa}(\bar{M}, \bar{R}, T_2) + \sigma_{\ln Sa}(\bar{M}, T_2) \times \rho_{\ln Sa(T_1),\ln Sa(T_2)} \times \bar{\epsilon}(T_1) \quad \text{Eq. (5)}$$

where T_1 is the reference period of interest; T_2 is the other periods in the CMS; T_{min} and T_{max} are the smaller and larger of T_1 and T_2; $\mu_{\ln Sa(T_2)}$ is the median (scenario specific) response spectrum presented in the natural logarithm scale; and $\sigma_{\ln Sa}$ is the log standard deviation.

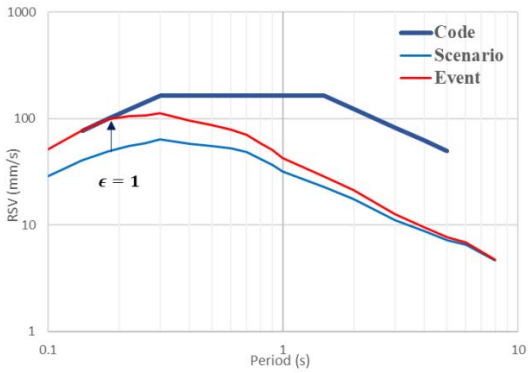

(a) T* = 0.18 s

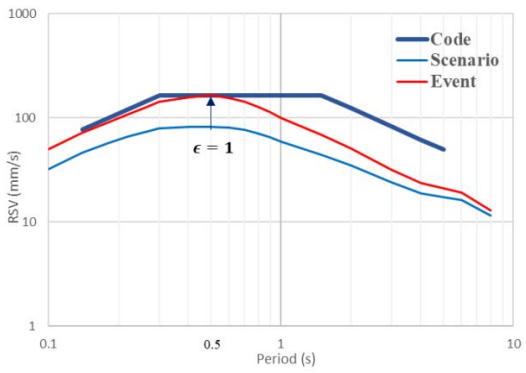

(b) T* = 0.5 s

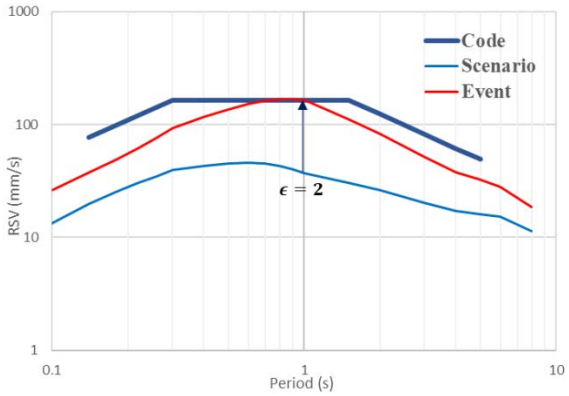

(c) T* = 1 s

Figure 7 Scenario Specific and Event Specific Spectra (GMPE Weighting Scheme 1)

3. ROCK ACCELEROGRAMS AND DISCUSSION

The CMSs that were presented in Section 2 were input into the ground motion database of NGA-West2 (2014) of the Pacific Earthquake Engineering Research (PEER) Center to retrieve and scale accelerogram records. In addition to specifying the target spectrum, other searching criteria included the style of faulting, magnitude and distance ranges, the shear wave velocity range ($V_{S,30}$) consistent with conditions on bedrock, and the criterion for determining the best match of the recorded response spectra with the target spectrum. This type of input information is summarized as follows:

- Style of faulting: Reverse/Oblique (typical of intraplate earthquakes);
- Magnitude range: M4 to M7;
- Joyner-Boore distance R_{jb} (defined as distance to the fault projection to the surface): 10 to 150 km;
- $V_{S,30}$: 600 m/s to 1800 m/s. representing rock conditions
- Criterion for best match: achieve a minimum residual based on taking *Square-Root-of-the-Sum-of-the-Squares* (SRSS) of deviations from the targeted spectrum over the period range of 0.05s to 2s.

The CMSs presented herein are only for the reference period of 0.5s as shown in Figures 8a – 8c. It is shown that CMSs based on the three weighting schemes (as defined in Table 4) are within 10% difference for natural periods of up to 1s (refer Table 5 for the listing of the scaling factors corresponding to each scheme). The robustness of the constructed CMSs (red color lines) is evident. Superposed on each of the CMS is the ensemble average of the scaled records (blue color lines). The inter-scheme comparison is also presented in Figure 9a (for the CMSs) and Figure 9b (ensemble averages) in the natural scale. CMSs for other reference periods can be found in Appendix B.

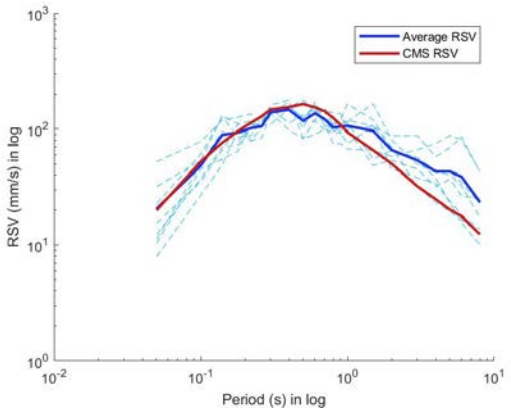

(a) Scheme 1

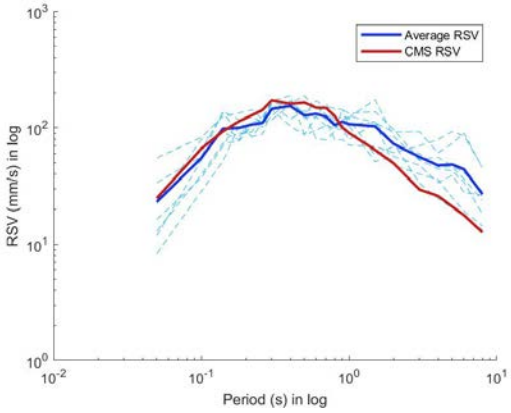

(b) Scheme 2

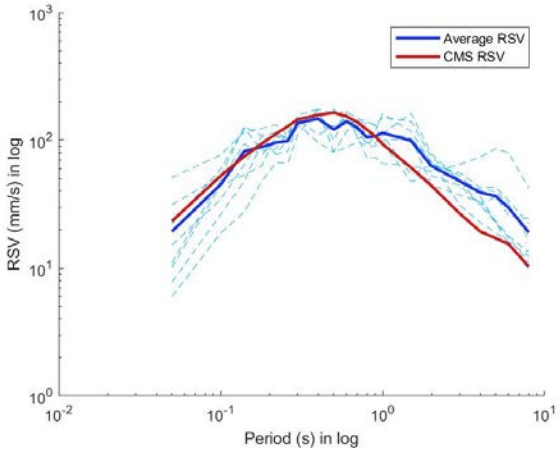

(c) Scheme 3

Figure 8 Conditional Mean Spectra and Ensemble Averaged Spectra in Velocity Format for T^* = 0.5 s

Given the CMS for T^*= 0.5s (for Scheme 2 weighting) and the other input information to the PEER database as presented in the above, an ensemble of accelerogram records that have been sourced and scaled from the database have been retrieved (Figure 10). Details of the earthquake events associated with the retrieved records are listed in Table 5.

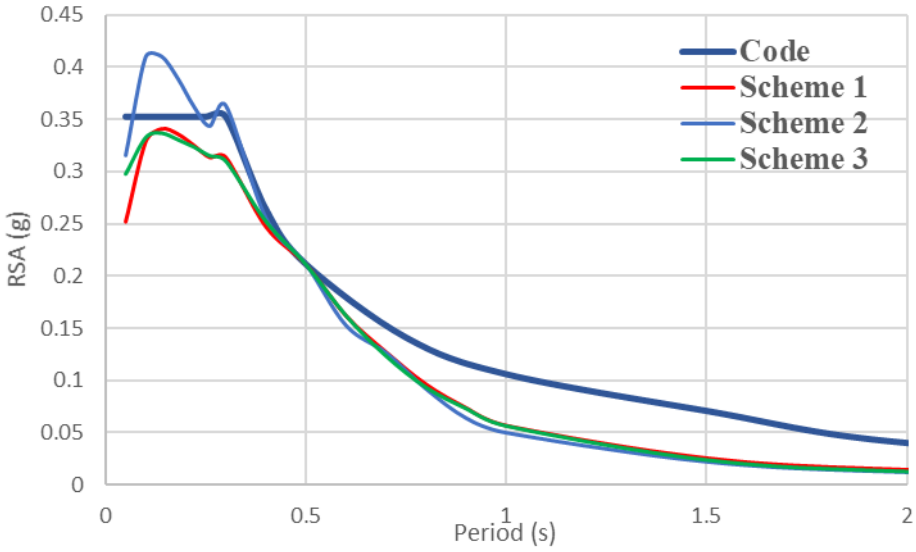

(a) Conditional Mean Spectra

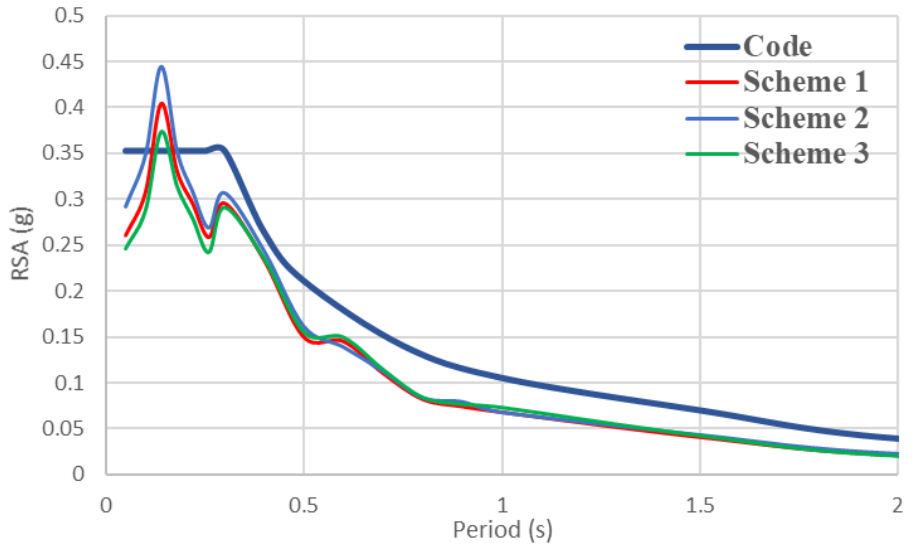

(b) Ensemble Averaged Response Spectra

Figure 9 Inter-scheme comparison of the Conditional Mean Spectra and Ensemble Averaged Response Spectra for $T^* = 0.5$ s

Table 5 Earthquake Events Detailed Summary

Earthquake	Year	Station	Magnitude	Rrup (km)	SF1[1]	SF2	SF3
"San Fernando"	1971	"Lake Hughes #4"	6.6	25.1	1.00	1.01	0.98
"San Fernando"	1971	"Lake Hughes #9"	6.6	22.6	1.35	1.37	1.33
"Northridge-01"	1994	"Lake Hughes #4 - Camp Mend"	6.7	31.7	1.23	1.25	N/A

"Chi-Chi_ Taiwan-05"	1999	"HWA031"	6.2	40.0	1.37 1.45[2]	1.38 1.47	1.34 1.42
"Chi-Chi_ Taiwan-05"	1999	"HWA035"	6.2	34.4	N/A	N/A	1.48
"Niigata_ Japan"	2004	"NIGH10"	6.6	39.4	1.06 0.64	1.07 0.65	1.04 0.63
"Chuetsu-oki_ Japan"	2007	"Joetsu_ Aramaki District"	6.8	32.5	N/A	0.57	N/A
"Chuetsu-oki_ Japan"	2007	"Nagano Togakushi"	6.8	78.9	0.79	N/A	0.77

[1] SF1 refers to Scaling Factor for *Scheme 1*

[2] Two scaling factor (SF) values in the same cell represent the SF for the accelerograms in the North-South direction and that in the West-East direction, respectively.

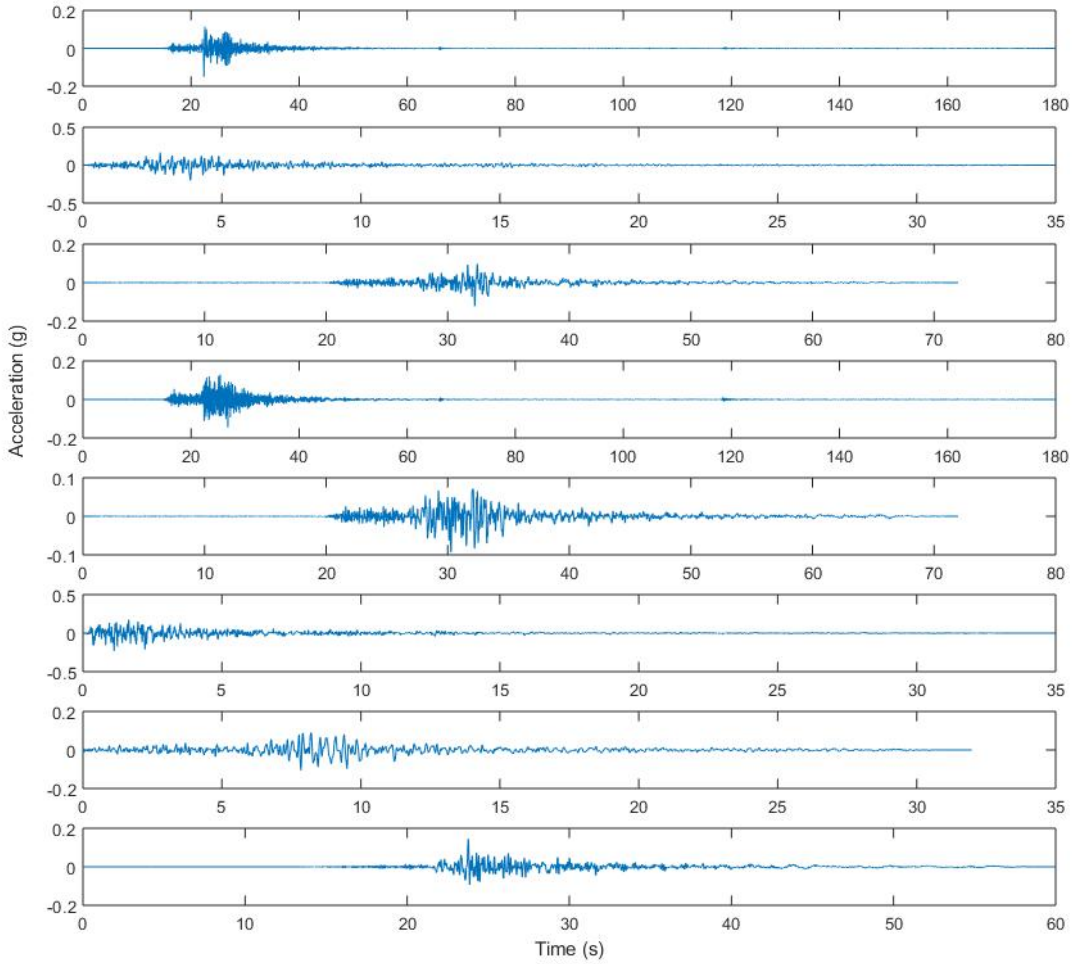

Figure 10 Bedrock Accelerograms Selected and Scaled from PEER database

4. SOIL AMPLIFICATION EFFECT AND SOIL SITE ACCELEROGRAMS

In this section, the soil amplification effect is analyzed with soil profiles generated from borehole records taken from capital cities in SEA. Equivalent linear one-dimensional response analysis was employed to compute the regolith site response using program SUA (Robinson, Dhu & Schneider, 2006), while detailed soil profile generating process and equivalent linear analysis were described in detail by Hu and co-works (2018). Three soil profiles, two of which are categorised as Class C site and the third one as Class D site, were analysed to generate soil site accelerograms using SUA. The bedrock accelerograms were those that had been selected and scaled using the CMS methodology presented in the earlier sections of the paper for weighting scheme *2* and reference period of 0.5 s. Relevant details of the soil profiles are summarised in Table 6 and the corresponding shear wave velocity profiles are shown in Figure 11. The borelog data can be found using the Dropbox link: https://www.dropbox.com/s/gg1pq88t7py6gyf/Soil%20Profile.xlsx?dl=0.

Table 6 Soil Properties for 3 Soil Profiles

Property	Soil 1	Soil 2	Soil 3
Location	Melbourne	Melbourne	Brisbane
depth to rock (m)	6.7	21.5	35.5
Mean SWV (m/s)	260.7	285.9	236.6
Period (s)	0.1	0.3	0.6
Rock SWV (m/s)	825	825	800
Soil Class	C	C	D

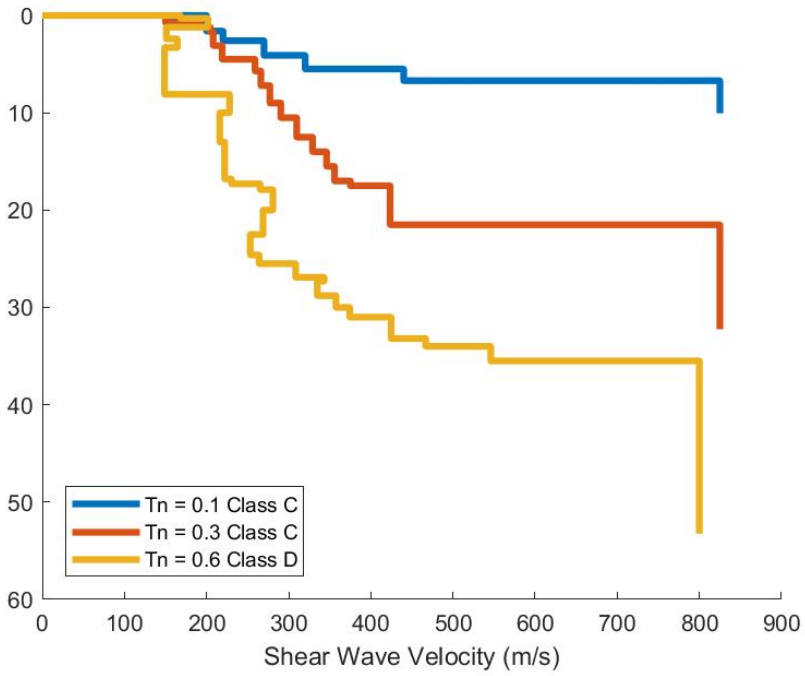

Figure 11 Soil Shear Wave Velocity Profiles

Response spectra in the velocity (RSV) format as calculated from SUA are shown in Figure 12a and 12b alongside the respective code models for site class C and D respectively. In both cases, the code models are shown to be exceeded in the low period range but overly conservative in the high period range.

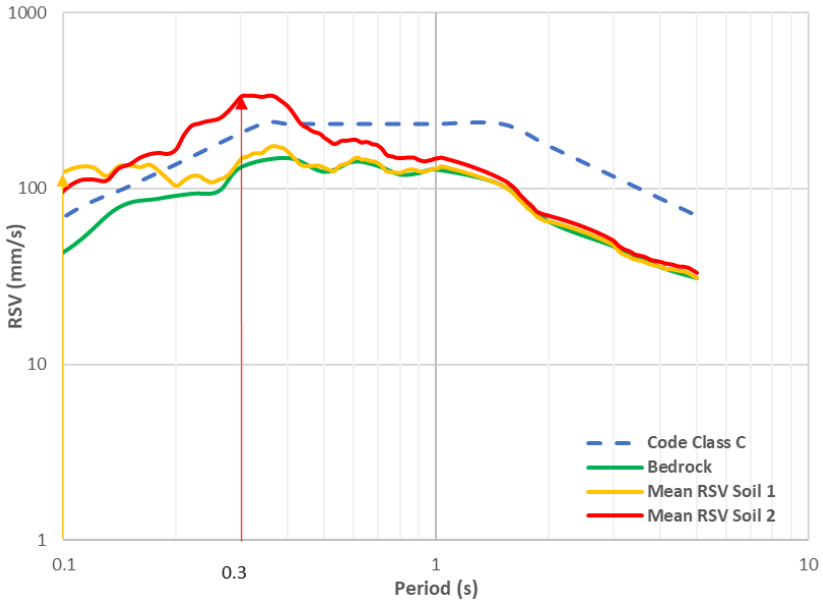

(a) Class C Site

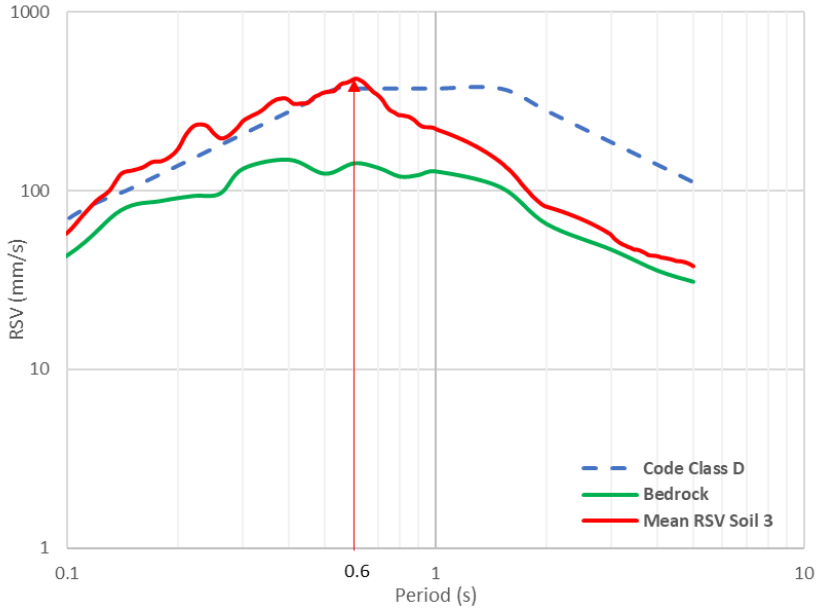

(b) Class D Site

Figure 12 Soil Site Velocity Response Spectra

5. CONCLUSION

This paper is about demonstrating the searching and scaling of accelerograms from the PEER database for simulating design earthquakes for use in the intraplate region of southeastern Australia (SEA). The design earthquake is based on a hazard factor of Kp Z= 0.12 which is the minimum level of hazard stipulated for Australia by the current edition of the Australian earthquake loading standard for a return period of 2500 years. The Conditional Mean Spectrum (CMS) methodology was employed for the spectral scaling of the accelerograms for bedrock conditions. The primary aim of this article is to demonstrate the adaptation of the CMS methodology for use in a stable region which is typified by a lack of indigenous strong motion records and uncertainties in the determination of the earthquake scenarios dominating site hazards. The Component Attenuation Model (CAM) was used as a tool to transform seismological models into GMPEs in order that the generic source factor of intraplate earthquakes (based on research findings in Eastern North America) could be combined with crustal modification factors that are representative of regional conditions. Predictions from CAM have been reconciled with a number of GMPEs including NGA-West2 models as well as models that had been developed locally from within Australia (and recognized by Geoscience Australia). In the absence of a PSHA that is associated with the code response spectrum the uniform seismicity model that had been developed by the authors was called up to constrain the dominating earthquake scenarios. Ground motion predictions for the dominating earthquake scenarios by multiple GMPEs including that of CAM were then combined using three alternative weighting schemes. As the generated CMSs were found to be insensitive to the adopted weighting scheme the robustness of the CMSs derived from the study became evident. Once the CMSs have been derived accelerograms have been retrieved and scaled from the PEER database to represent potential bedrock excitations consistent with the conditions of SEA and a return period of 2500 years. Program SUA was then employed to generate accelerograms on the surface of some example Class C and D soil sites.

ACKNOWLEDGEMENT

The support of the Commonwealth Australia through the Cooperative Research Centre program and the Australian Research Council Discovery Project (DP180101593) is gratefully acknowledged.

REFERENCE

Abrahamson, N. A., Silva, W. J., & Kamai, R. (2014). Summary of the ASK14 ground motion relation for active crustal regions. *Earthquake Spectra*, *30*(3), 1025-1055.

Allen, T. I. (2012). Stochastic ground-motion prediction equations for southeastern Australian earthquakes using updated source and attenuation parameters. *Geoscience Australia Record*, 69, 55.

Atkinson, G. M. (1993). Earthquake source spectra in eastern North America. *Bulletin of the Seismological Society of America*, 83(6), 1778-1798.

Atkinson, G. M. (2008). Ground-motion prediction equations for eastern North America from a referenced empirical approach: Implications for epistemic uncertainty. *Bulletin of the Seismological Society of America*, *98*(3), 1304-1318.

Atkinson, G. M., & Boore, D. M. (1995). Ground-motion relations for eastern North America. *Bulletin of the Seismological Society of America*, *85*(1), 17-30.

Atkinson, G. M., & Boore, D. M. (2006). Earthquake ground-motion prediction equations for eastern North America. *Bulletin of the seismological society of America*, *96*(6), 2181-2205.

Atkinson, G. M., & Silva, W. (2000). Stochastic modeling of California ground motions. *Bulletin of the Seismological Society of America*, 90(2), 255-274.

Atkinson, G. M., & Kaka, S. I. (2007). Relationships between felt intensity and instrumental ground motion in the central United States and California. *Bulletin of the Seismological Society of America*, 97(2), 497-510.

Baker, J. W., & Cornell, C. A. (2006). Correlation of response spectral values for multicomponent ground motions. *Bulletin of the seismological Society of America*, 96(1), 215-227.

Baker, J. W. (2010). Conditional mean spectrum: Tool for ground-motion selection. *Journal of Structural Engineering*, *137*(3), 322-331.

Baker, J. W. (2015, November). Ground motion selection for performance-based engineering, and the Conditional Mean Spectrum as a selection tool. In *Proceedings of the Tenth Pacific Conference on Earthquake Engineering Building an Earthquake-Resilient Pacific* (pp. 6-8).

Boore, D. M. (1983). Stochastic simulation of high-frequency ground motions based on seismological models of the radiated spectra. *Bulletin of the Seismological Society of America*, *73*(6A), 1865-1894.

Boore, D. M., Di Alessandro, C., & Abrahamson, N. A. (2014). A generalization of the double-corner-frequency source spectral model and its use in the SCEC BBP validation exercise. *Bulletin of the Seismological Society of America*, *104*(5), 2387-2398.

Campbell, K. W. (2003). Prediction of strong ground motion using the hybrid empirical method and its use in the development of ground-motion (attenuation) relations in eastern North America. *Bulletin of the Seismological Society of America*, *93*(3), 1012-1033.

Chiou, B. S. J., & Youngs, R. R. (2014). Update of the Chiou and Youngs NGA model for the average horizontal component of peak ground motion and response spectra. *Earthquake Spectra*, *30*(3), 1117-1153.

Drake, R. M., & Bachman, R. E. (1996). NEHRP provisions for 1994 for nonstructural components. *Journal of architectural Engineering*, *2*(1), 26-31.

Hu, Y., Lumantarna, E., Lam, N., Menegon, S., Wilson, J. (2018, November). Development of a soil site ground motion database for Australian seismic structural design. In *Proceedings of the 2018 Australian Earthquake Engineering Society Conference in Perth*.

Lam, N., Sinadinovski, C., Koo, R., & Wilson, J. (2003). Peak ground velocity modelling for Australian intraplate earthquakes. *Journal of Seismology and Earthquake Engineering*, 5(2), 11-22.

Lam, N. T., Tsang, H. H., Lumantarna, E., & Wilson, J. L. (2016). Minimum loading requirements for areas of low seismicity. *Earthquakes and Structures*, 11(4), 539-561.

Lam, N., Wilson, J., Chandler, A., & Hutchinson, G. (2000). Response spectral relationships for rock sites derived from the component attenuation model. *Earthquake engineering & structural dynamics*, 29(10), 1457-1489.

Lam, N., Wilson, J., & Tsang, H. H. (2010). Modelling earthquake ground motions by stochastic method. Stochastic control, 475-492.

Lumantarna, E., Wilson, J. L., & Lam, N. T. K. (2012). Bi-linear displacement response spectrum model for engineering applications in low and moderate seismicity regions. *Soil Dynamics and Earthquake Engineering*, 43, 85-96.

McCue, K. (1995). Atlas of Isoseismal Maps of Australian Earthquakes, Australian Geological Survey, Org.

Ogweno, L. P., & Cramer, C. H. (2014). Comparing the CENA GMPEs using NGA-East ground-motion database. *Seismological Research Letters*, 85(6), 1377-1393.

Pezeshk, S., Zandieh, A., & Tavakoli, B. (2011). Hybrid empirical ground-motion prediction equations for eastern North America using NGA models and updated seismological parameters. *Bulletin of the Seismological Society of America*, *101*(4), 1859-1870.

Robinson, D., Dhu, T., & Schneider, J. (2006). SUA: A computer program to compute regolith site-response and estimate uncertainty for probabilistic seismic hazard analyses. *Computers & geosciences*, *32*(1), 109-123.

Shahjouei, A., & Pezeshk, S. (2015). Hybrid empirical ground-motion model for central and eastern North America using hybrid broadband simulations and NGAWest2 GMPEs. *NGA-East: Median Ground-Motion Models for the Central and Eastern North America Region, PEER Report Number 2015, 4*.

Somerville, P., Graves, R., Collins, N., Song, S. G., Ni, S., & Cummins, P. (2009, December). Source and ground motion models for Australian earthquakes. In *Proc. 2009 Annual Conference of the Australian Earthquake Engineering Society* (pp. 11-13).

Standard, A. (2007). AS1170. 4. *Structural Design Actions, Part, 4*.

Tang, Y., Lam, N., Tsang, H. H., & Lumantarna, E. (2019). Use of Macroseismic Intensity Data to Validate a Regionally Adjustable Ground Motion Prediction Model. *Geosciences*, *9*(10), 422.
Standards Australia. 2007. *AS 1170.4-2007: Structural design actions, Part 4: Earthquake actions in Australia*. Sydney, NSW: SAI Global.

Yenier, E., & Atkinson, G. M. (2015). Regionally adjustable generic ground-motion prediction equation based on equivalent point-source simulations: Application to central and eastern North America. *Bulletin of the Seismological Society of America*, *105*(4), 1989-2009.

Appendix A

In Appendix A the approach to construct response spectra using the simplified CAM-PGV version is presented with several examples in various earthquake scenarios. This approach and the coefficients were introduced by Tang and his co-worker (2019). As a simplified version, this CAM-PGV model is able to calculate the Peak Ground Velocity (PGV), an important indicator of structural damage, with earthquake magnitude, source-to-site distance and site conditions. The full version of CAM can generate acceleration response spectrum directly and is available from this link: https://www.dropbox.com/s/zct2jkdyt6q06w9/CAM%20Manual.docx?dl=0.

CAM as a GMPE expresses PGV in an additive logarithmic (base 10) format by decoupling the source and attenuation effects into different components as shown in Eq. (A1).

$$logY = log\Delta + log\alpha + log\beta + logG + log\gamma_{uc} + logC \quad \text{Eq. (A1)}$$

Where Y is the predicted mean PGV assuming 5% damping; ; Δ is the referenced PGV defined as the PGV in hard-rock condition (no or minor crustal effect) under the referenced scenario ($M = 6, R = 30\ km$); α is the source factor expressed as a function of earthquake magnitude and Brune's stress parameter, as in Eq. (A2); β is the path factor excluding the geometric attenuation factor which is accounted for by G, and these factors are covered in Eq. (A3) - (A4); γ_{uc} is the crustal effect including three components explained in Section 2.1, i.e. the upper crust amplification effect γ_{am}, the attenuation of the upper crust γ_{an} and the mid crust modification effect γ_{mc} ($\gamma_{uc} = \gamma_{am} \times \gamma_{an} \times \gamma_{mc}$). The equations to calculate these three components are presented in Eq. (A5) - (A7); and C is the calibration factor to minimize discrepancies between the model predictions and simulation results, as in Eq. (A8).

$$log\alpha = a_1 \times M^{a_2} \times \Delta\sigma^{a_3} + a_4 \quad \text{Eq. (A2)}$$

$$log\beta = (b_1 \times M + b_2) \times {Q_0}^{b_3} \times (logR)^{b_4} + b_5 \quad \text{Eq. (A3)}$$

$$G = \frac{G_R}{G_{30}} \quad \text{Eq. (A4)}$$

$$log\gamma_{am} = \gamma_1 \times M^{\gamma_2} \times {V_{s,30}}^{\gamma_3} + \gamma_4 \times V_{s,30} \quad \text{Eq. (A5)}$$

$$log\gamma_{an} = \gamma_5 \times M^{\gamma_6} \times {\kappa_0}^{\gamma_7} + \gamma_8 \quad \text{Eq. (A6)}$$

$$log\gamma_{mc} = (\frac{\rho_{sim}}{\rho_s}) \times (\frac{\beta_{0_{sim}}}{\beta_{0_s}})^{-0.273 \times M + 3.278} \quad \text{Eq. (A7)}$$

$$logC = c_1 \times R^4 + c_2 \times R^3 + c_3 \times R^2 + c_4 \times R + c_5 \quad \text{Eq. (A8)}$$

Where $\Delta\sigma$ is the Brune's stress parameter; Q_0 is the regional dependent quality factor for wave transmission ; R is the hypocentral distance and $R = \sqrt{{R_{rup}}^2 + (10^{-0.405+0.235\times M})^2}$ (Yenier & Atkinson, 2015) to simulate the near-distance saturation effects; G_R is the geometric term at hypocentral distance R, where the geometric spreading rate in this study employs $G_R = R^{-1}$ in

the distance range $0-70\,km$, $G_R = 70^{-1}$ in the distance range $70-130\,km$, $G_R = 70^{-1} \times (\frac{R}{130})^{-0.5}$ for longer distances; G_{30} is the geometric term at $R_{rup} = 30\,km$; $V_{s,30}$ is the average shear wave velocity in the upper 30 meters of the crust; κ_0 is the shape factor to diminish spectral amplitudes at high frequencies; $\rho_{sim} = 2.8\,g/cm^3$, $\beta_{0_{sim}} = 3.8km/s$, are the benchmark density and shear wave velocity of hard rock conditions; ρ_s (normally takes $2.8\,g/cm^3$) and β_{0_s} are the density and shear wave velocity of site crust at the depth of the source (i.e. the mid-crust).

The coefficients for computing PGV are summarised in Table A1 and a spreadsheet for readers' application of CAM-PGV is ready for downloading from this link: https://www.dropbox.com/s/amg8ysn9orwpxxe/CAM-PGV%20Demo.xlsx?dl=0. Based on the recommendations from Tang et al. (2019) and Lam et al. (2003), the seismological parameters for SEA are summarised in Table A2. The velocity response spectrum can be constructed from PGV in trilinear form in logarithmic scale. An example of such spectrum is demonstrated in Figure A1 and the steps to generate it are described below.

Table A1 Coefficients for modelling PGV using CAM-PGV

$\log \alpha$	Δ (mm/s)	a_1	a_2	a_3	a_4
	390	27.797	0.08414	0.0059	-33.35
$\log \beta$	b_1	b_2	b_3	b_4	b_5
	0.06287	-0.6326	-0.4963	4.431	0.06135
$\log C$	c_1	c_2	c_3	c_4	c_5
	0.01714	-0.06931	0.08404	-0.09224	0.0876
$\log \gamma_{am}$	γ_1	γ_2	γ_3	γ_4	
	0.7334	-0.5251	-0.8479	-0.019	
$\log \gamma_{an}$	γ_5	γ_6	γ_7	γ_8	
	-21.35	-1.351	0.5584	-0.03336	

Table A2 Recommended Seismological Parameters in SEA

Parameter	$\Delta\sigma$ (bar)	Q_0	$V_{s,30}$ (m/s)	κ_0 (s)	V_8 (km/s)
Recommended Value	200	200	760	0.033	3.5

The velocity response spectrum consists of three parts, the acceleration-, velocity- and displacement-controlled regions, which are divided by two corner periods. The lower corner period is typically taken as 0.3 seconds and the higher corner period is magnitude-dependent and can be computed with Eq. (A9) (Lumantarna, Wilson & Lam, 2012). Between the two corner periods is the velocity-controlled region, where RSV is constant at value RSV_{max} and can be calculated as Eq. (A10) using PGV determined from the CAM-PGV model. Similarly, in the acceleration- and displacement-controlled regions, the acceleration and displacement are constant at RSA_{max} and RSD_{max}, respectively. The equations to calculate the max response acceleration RSA_{max} and displacement RSD_{max} are presented in Eq. (A11) – (A12).

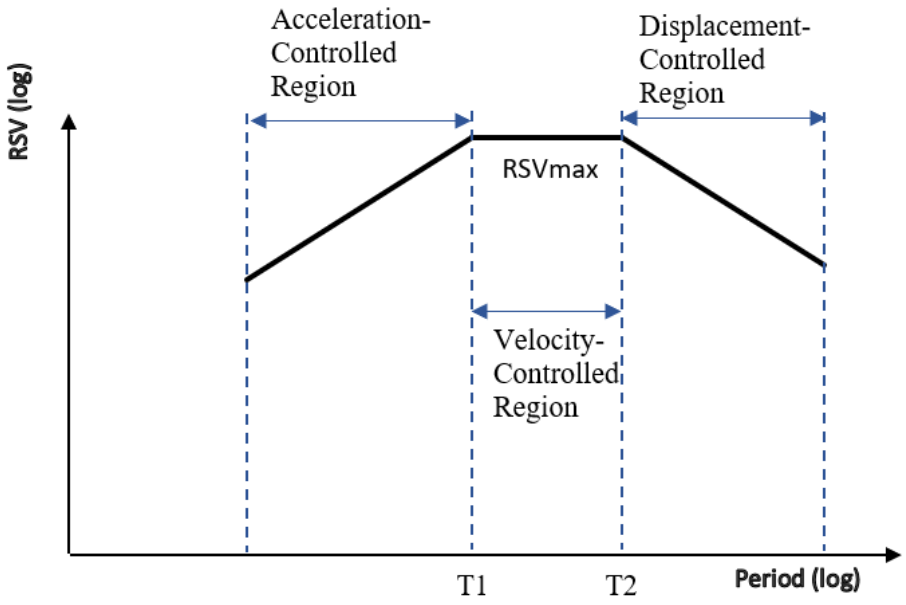

Figure A1 Trilinear Velocity Response Spectrum in Logarithmic Scale

$$T_2 = 0.5 + \frac{(M-5)}{2} \quad \text{Eq. (A9)}$$

$$RSV_{max} = PGV \times 1.8 \quad \text{Eq. (A10)}$$

$$RSA_{max} = RSV_{max} \times \frac{2\pi}{T_1} \quad \text{Eq. (A11)}$$

$$RSD_{max} = RSV_{max} \times \frac{T_2}{2\pi} \quad \text{Eq. (A12)}$$

Then the velocity response spectrum can be constructed as RSV is proportional to period T in the acceleration-controlled region and inversely proportional to period T in the displacement-controlled region, as following:

$$\begin{cases} T \le T_1 & RSV = RSA_{max} \times \frac{T}{2\pi} \\ T_1 < T < T_2 & RSV = RSV_{max} \\ T \ge T_2 & RSV = RSD_{max} \times \frac{2\pi}{T} \end{cases} \quad \text{Eq. (A13)}$$

Three examples are illustrated in Figure A2 to demonstrate the performance of CAM-PGV under 3 scenarios, which are small events at short distance scenario; referenced scenario; and large event at long distance scenario.

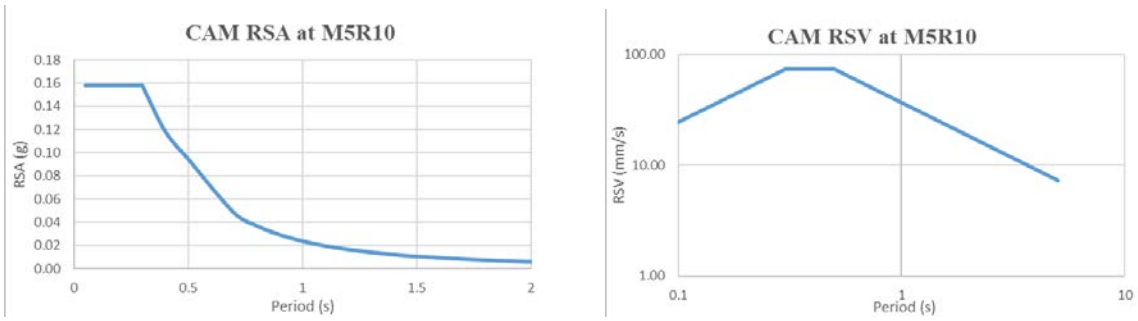

(a) Scenario 1 M = 4, R = 10 km

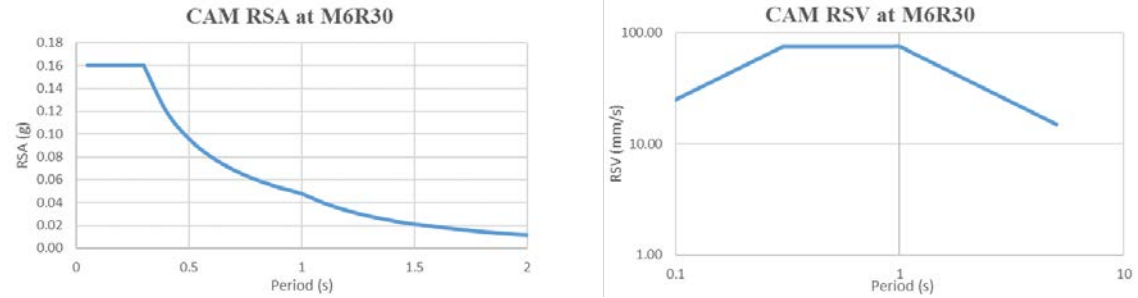

(a) Scenario 2 M = 6, R = 30 km

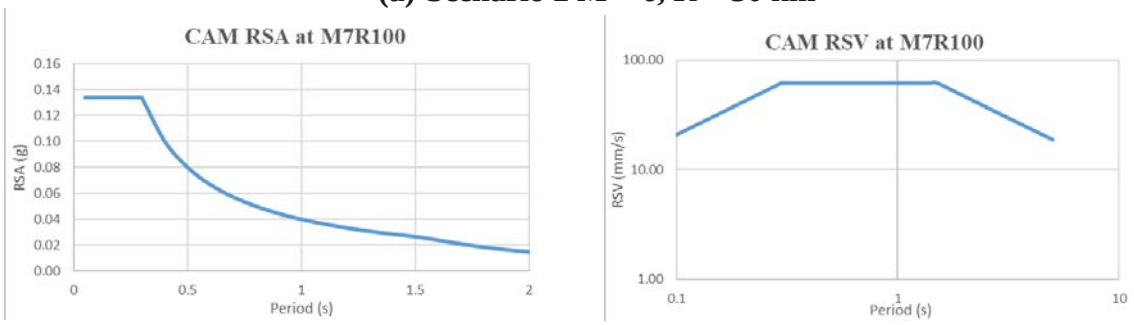

(a) Scenario 3 M = 7, R = 100 km

Figure A2 Performance of CAM-PGV in 3 Scenarios

Appendix B

Appendix B includes the response spectral acceleration values at period of interest being 0.18s, 0.5s and 1s that envelope the CMS RSA values calculated from *Scheme 1, 2 & 3*. The bedrock ground motion acceleration selected and scaled based on these spectra can be downloaded from this link: https://www.dropbox.com/s/mw1sax9yhdzjqo5/Bedrock%20Accelerograms.xlsx?dl=0.

Table B1 Response Spectral Acceleration Value (g) at Three Periods of Interest

T (s)	Period of Interest (s)		
	0.18	**0.5**	**1**
0.05	0.295	0.318	0.103
0.1	0.360	0.424	0.157
0.14	0.369	0.426	0.172
0.18	0.353	0.405	0.174
0.22	0.307	0.373	0.181
0.26	0.268	0.351	0.190
0.3	0.239	0.368	0.199
0.4	0.158	0.258	0.188
0.5	0.113	0.211	0.175
0.6	0.086	0.164	0.163
0.7	0.064	0.136	0.150
0.8	0.048	0.101	0.134
0.9	0.037	0.077	0.119
1	0.029	0.060	0.106
1.5	0.012	0.028	0.048
2	0.007	0.016	0.027
3	0.003	0.007	0.011
4	0.002	0.004	0.006
5	0.001	0.003	0.004
6	0.001	0.002	0.003
8	0.000	0.001	0.001